NeuroImage 188 (2019) 557–571

Contents lists available at ScienceDirect

NeuroImage

journal homepage: www.elsevier.com/locate/neuroimage

Cortical dynamics during preparation and execution of reactive balance responses with distinct postural demands

Teodoro Solis-Escalante [a,b,*], Joris van der Cruijsen [a,b,c], Digna de Kam [b,d], Joost van Kordelaar [a,e], Vivian Weerdesteyn [b,f,1], Alfred C. Schouten [a,e,1]

[a] Department of Biomechanical Engineering, Delft University of Technology, Delft, the Netherlands
[b] Department of Rehabilitation, Donders Institute for Brain, Cognition and Behavior, Radboud University Medical Center, Nijmegen, the Netherlands
[c] Department of Rehabilitation Medicine, Erasmus Medical Center, Rotterdam, the Netherlands
[d] Department of Bioengineering, Swanson School of Engineering, University of Pittsburgh, Pittsburgh, PA, USA
[e] Department of Biomechanical Engineering, Faculty of Engineering Technology, Technical Medical Centre, University of Twente, Enschede, the Netherlands
[f] Sint Maartenskliniek Research, Nijmegen, the Netherlands

ARTICLE INFO

Keywords:
Balance
Posture
Electroencephalogram (EEG)
Independent component analysis (ICA)
Mobile brain/body imaging (MOBI)

ABSTRACT

The contributions of the cerebral cortex to human balance control are clearly demonstrated by the profound impact of cortical lesions on the ability to maintain standing balance. The cerebral cortex is thought to regulate subcortical postural centers to maintain upright balance and posture under varying environmental conditions and task demands. However, the cortical mechanisms that support standing balance remain elusive. Here, we present an EEG-based analysis of cortical oscillatory dynamics during the preparation and execution of balance responses with distinct postural demands. In our experiment, participants responded to backward movements of the support surface either with one forward step or by keeping their feet in place. To challenge the postural control system, we applied participant-specific high accelerations of the support surface such that the postural demand was low for stepping responses and high for feet-in-place responses. We expected that postural demand modulated the power of intrinsic cortical oscillations.

Independent component analysis and time-frequency domain statistics revealed stronger suppression of alpha (9–13 Hz) and low-gamma (31–34 Hz) rhythms in the supplementary motor area (SMA) when preparing for feet-in-place responses (i.e., high postural demand). Irrespective of the response condition, support-surface movements elicited broadband (3–17 Hz) power increase in the SMA and enhancement of the theta (3–7 Hz) rhythm in the anterior prefrontal cortex (PFC), anterior cingulate cortex (ACC), and bilateral sensorimotor cortices (M1/S1). Although the execution of reactive responses resulted in largely similar cortical dynamics, comparison between the bilateral M1/S1 showed that stepping responses corresponded with stronger suppression of the beta (13–17 Hz) rhythm in the M1/S1 contralateral to the support leg. Comparison between response conditions showed that feet-in-place responses corresponded with stronger enhancement of the theta (3–7 Hz) rhythm in the PFC. Our results provide novel insights into the cortical dynamics of SMA, PFC, and M1/S1 during the control of human balance.

1. Introduction

Balance control is a complex motor task controlled by neural ensembles in the spinal cord, brainstem, cerebellum, and cerebral cortex (Nutt et al., 2011; Takakusaki, 2017). Although early animal studies suggested limited participation of the cerebral cortex in controlling balance and posture (Magnus, 1926; Sherrington, 1910), recent evidence from human studies indicates that the cerebral cortex may regulate the excitability of subcortical postural centers to maintain balance and postural stability according to environmental demands (Bohnen and Jahn, 2013; Jahn and Zwergal, 2010; Peterson and Horak, 2016). Yet, there is limited knowledge about the contributions from different cortical areas to balance control (Bolton, 2015; Jacobs, 2014).

Previous EEG studies on balance control have mainly focused on the

* Corresponding author. Department of Biomechanical Engineering, Delft University of Technology, Delft, the Netherlands.
E-mail address: teodoro.solisescalante@radboudumc.nl (T. Solis-Escalante).
[1] These authors contributed equally.

https://doi.org/10.1016/j.neuroimage.2018.12.045
Received 26 September 2018; Received in revised form 7 December 2018; Accepted 21 December 2018
Available online 24 December 2018

analysis of scalp-level event-related potentials elicited by whole-body mechanical perturbations to standing balance (see Varghese et al. (2017); Wittenberg et al. (2017) for recent reviews), whereas only few studies have investigated the scalp-level spectral characteristics of cortical activity elicited by such perturbations (Mierau et al., 2017; Varghese et al., 2014). Cortical dynamics are oscillatory in nature (Basar et al., 1999) and are thought to represent the balance between neuronal excitation and inhibition in the brain (Buzsáki et al., 2012; Muthukumaraswamy, 2014). In particular, inhibitory GABAergic interneurons are highly relevant for shaping the behavior of the large neuronal groups that give rise to the oscillatory characteristics (i.e., frequency and amplitude) of the EEG (Gaetz et al., 2011; Hall et al., 2011; Muthukumaraswamy, 2014). Further insights into the cortical control of balance can be gained when considering the spectral characteristics of perturbation-related cortical activity. Time-frequency analysis of the EEG can reveal changes to specific cortical dynamics in relation to internal and external events (Makeig, 1993; Pfurtscheller and Lopes da Silva, 1999). In turn, different rhythms have been associated with distinct cognitive and sensorimotor functions. In particular, low-frequency cortical rhythms (<13 Hz) are associated with perception and cognitive control (Cavanagh and Frank, 2014; Klimesch, 1999), whereas high-frequency cortical rhythms (>13 Hz) are commonly associated with motor function (Engel and Fries, 2010; Muthukumaraswamy, 2010; Neuper and Pfurtscheller, 2001).

Nonetheless, previous ERP-based studies provide evidence that suggest various concurrent sensorimotor and cognitive processes related to the initial phases of balance control. Mechanical perturbations to standing balance elicit the robust negative potential N1 (latency: 85–163 ms, amplitude: −0.8 to −80 μV) distributed over frontal, central, and parietal scalp sites (Varghese et al., 2017). Currently, there is no consensus on the functional role of the N1 potential (Varghese et al., 2017). On one hand, the N1 potential has been suggested to represent the processing of sensory information for the purpose of coordinating reactive balance responses (Dietz et al., 1984, 1985; Dimitrov et al., 1996; Quant et al., 2004; Staines et al., 2001). On the other hand, the N1 potential could represent an error signal for the detection of postural instability (Adkin et al., 2006, 2008; Mochizuki et al., 2009). The role of the N1 potential as an error signal is supported by studies showing that the N1 potential is affected by the predictability and the postural threat of a given balance perturbation, i.e., the amplitude of the N1 potential decreases as the predictability of a balance perturbation increases (Adkin et al., 2006, 2008; Mochizuki et al., 2010) and increases as the perceived postural threat increases (Adkin et al., 2008; Mochizuki et al., 2010). Inverse mapping of the N1 potential indicates that it likely originates from the supplementary motor area (SMA) (Marlin et al., 2014), with contributions of the anterior cingulate cortex (ACC) and the posterior parietal cortex (PPC) (Mierau et al., 2015). Time-frequency analyses of the EEG following mechanical perturbations to standing balance have shown transient power increase of theta (4–7 Hz), alpha (8–12 Hz), and beta (13–30 Hz) rhythms that matches the latency and location of the N1 potential (Mierau et al., 2017; Varghese et al., 2014). The evidence found in previous studies indicates that the scalp-level N1 potential represents various concurrent sensorimotor and cognitive processes distributed across multiple cortical areas.

In addition, studies that focused on preparatory processes prior to a mechanical perturbation demonstrated a slow negative shift of the cortical potential (contingent negative variation, CNV) and sustained power decrease of alpha and beta rhythms over fronto-central electrode sites (Jacobs et al., 2008; Mochizuki et al., 2008; Smith et al., 2012). These phenomena typically represent cortical mechanisms of motor preparation (Neuper and Pfurtscheller, 2001; van Rijn et al., 2011) arising from the SMA, the prefrontal cortex (PFC), the sensorimotor cortices (M1/S1) (Hamano et al., 1997; Ohara et al., 2000), the basal ganglia (Rektor et al., 2005), and (sub)thalamic nuclei (Klostermann et al., 2007). Yet, it is currently unclear whether the CNV or the alpha and beta power decrease have a specific contribution to the preparation of balance responses (Mochizuki et al., 2010; Smith et al., 2014).

To gain further insight into the cortical mechanisms of balance control, we analyzed high-density EEG recorded during preparation and execution of reactive balance responses. Our goal was to determine the source-level cortical oscillatory dynamics of preparatory and reactive balance control, and how these are modulated by the postural demand of the reactive balance response. We relied on advanced processing of high-density EEG, combining blind source separation algorithms and source localization techniques to reveal EEG source-level dynamics during whole-body movement (Gramann et al., 2014; Makeig et al., 2009), while reducing physiological noise and movement artifacts (Gwin et al., 2010; Kline et al., 2015; Oliveira et al., 2016). We recorded high-density EEG in an experiment where participants anticipated and responded to high-intensity backward translations of the support surface. We studied two distinct behavioral responses with different postural demands, namely, maintaining balance by making one corrective step (low postural demand) or by keeping their feet in place (high postural demand). High-intensity balance perturbations can be overcome using feet-in-place strategies with great effort, while making a corrective step is a natural, less demanding reaction (de Kam et al., 2016). The key novelty of our study is the direct comparison of the two response conditions elicited by identical balance perturbations, which allowed us to investigate task-specific differences in cortical dynamics related to top-down processes of preparatory and reactive balance control, separately from cortical activity evoked by sensory afferences from the imposed mechanical perturbation.

Our hypothesis was that higher postural demand requires stronger modulation of cortical oscillations from SMA, ACC, and PPC with feet-in-place responses. Additionally, because late phases of reactive balance responses may be cortically mediated (Jacobs and Horak, 2007; Maki and McIlroy, 2007), we expected that lateralized activity in the sensorimotor cortices (M1/S1, alpha and beta rhythms) would reflect the asymmetric postural behavior of stepping responses.

2. Materials and methods

2.1. Participants

Ten healthy volunteers participated in this study (age: 24.2 ± 3.6 years; four women). All volunteers gave written informed consent prior to their participation. None of the participants had previous history of neurological or neuromuscular disease, or any other impairments that limited their involvement in the experiment. The experimental procedure was approved by the ethics committee of the Medisch Spectrum Twente (Enschede, The Netherlands; NL52632.044.15). The experiments were conducted in accordance with The Declaration of Helsinki.

2.2. Experimental design

The experiments were conducted with the Radboud Falls Simulator, a dynamic posturography system for investigating standing balance (Nonnekes et al., 2013). During the experiments, the participants stood in the middle of a movable platform, wearing a safety harness attached to the ceiling via a moving suspension that follows the platform movements. The task of the participants was to maintain an upright posture and to respond to balance perturbations, imposed by sudden translations of the movable platform. Fig. 1 illustrates the experimental setup.

The experimental session began by determining a participant-specific stepping threshold (de Kam et al., 2016), which is defined as the maximum acceleration of the movable platform that can be overcome without stepping in one out of three trials. During this procedure, the acceleration was gradually increased from 0.875 m/s^2, in increments of 0.125 m/s^2, until a stepping reaction was elicited. Then, the same acceleration was tested with two additional trials. In case the three trials elicited stepping reactions, the acceleration was decreased one level and tested with two additional trials. The mean stepping threshold of the

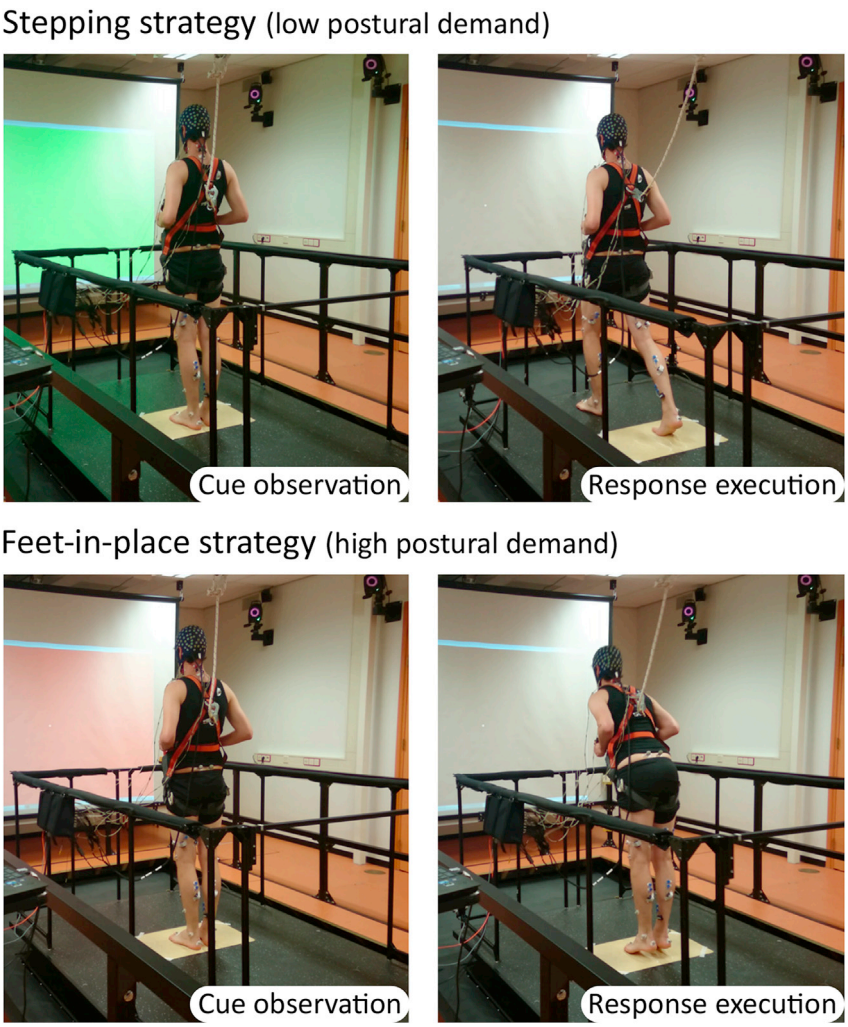

Fig. 1. *Experimental setup*. Participants stood on a movable platform wearing a safety harness and an electrode cap. Their task was to respond to balance perturbations using stepping or feet-in-place responses. The required response was indicated by visual cues. The balance perturbations were backward movements of the support surface at the individual maximum acceleration that could be overcome without stepping.

participants was 1.58 m/s^2 (standard deviation: 0.35 m/s^2; range: 1.05–2.25 m/s^2). The stepping threshold was only determined for backward movement of the support surface. For this part of the experimental session, the participants were verbally instructed to maintain their balance by keeping their feet in place.

In the main experiment, the participants responded to backward movements of the support surface (at the acceleration of the participant-specific stepping threshold) using either stepping or feet-in-place responses, as indicated by visual cues. The experiment included 50 trials per condition, divided into five blocks of 20 trials. The order of the trials was randomized within each block, to maintain the probability of both conditions at 50%. To prevent fatigue, short pauses lasting 3–5 min were allowed between blocks. Prior to the experiment, participants practiced during an additional block of 20 trials to familiarize themselves with the task and to ensure that they were able to maintain standing balance with feet-in-place responses when requested. The familiarization trials were not included in the analysis. Each trial included three phases, namely, cue observation, response preparation, and response execution. Fig. 2 illustrates the timing of these phases and the events occurring within a trial.

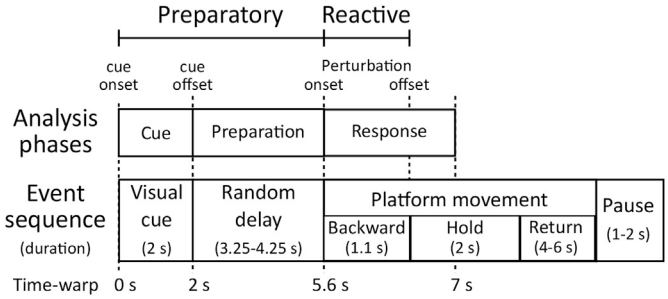

Fig. 2. *Experimental paradigm: event sequence and durations.* At the beginning of each trial, a visual cue indicated which response to use for maintaining standing balance. The visual cue was followed by an interval of random duration. Participants stood quietly on the platform, maintaining a natural upright posture. This interval terminated with the onset of the balance perturbation (backward movement of the support surface). The perturbation consisted of three phases: acceleration (300 ms), constant velocity (500 ms), and deceleration (300 ms). Afterwards, the platform remained stationary before returning to its initial position at the end of a trial. A new trial started after a short pause. Duration of the random pauses was drawn from an uniform distribution. For analysis, each trial was divided into three phases: cue observation, response preparation, and response execution. The bottom line indicates the time-warped duration of these three phases.

2.3. Data acquisition

We recorded high-density EEG using a cap with 126 Ag-AgCl electrodes (WaveGuard, ANT Neuro, The Netherlands). The electrodes in the

cap were distributed across the scalp according to the five percent electrode system (Oostenveld and Praamstra, 2001). The EEG was referenced to the common average during acquisition. The ground electrode was placed on the left mastoid. A biosignal amplifier (REFA System, TMSi, The Netherlands) recorded the EEG at 2048 Hz without any filters, except for a built-in antialiasing low-pass filter (552 Hz). To monitor for physiological artifacts, the same amplifier recorded electrical activity of the left eye (electrooculogram, EOG) and the neck muscles (electromyogram, EMG) using adhesive Ag-AgCl electrodes. The EOG was recorded from electrodes placed slightly above the nasion (vertical eye movement) and at the outer cantus of the left eye (horizontal eye movement). The EMG was recorded using four bipolar derivations placed on the left and right sternocleidomastoid muscles and the upper part of the left and right trapezius muscle (just below the hairline at the back of the head). Ground reaction forces were recorded from two force plates (AMTI Custom 6 axis composite force platform, USA; size: 60 × 180 cm each; sampling rate: 2000 Hz) embedded in the moveable platform. Synchronization triggers were generated by the platform controller and recorded together with the EEG signals. Task performance was visually evaluated and manually annotated during data acquisition.

2.4. EEG analysis

2.4.1. Preprocessing

The EEG data was analyzed with MATLAB (The Mathworks, Inc., USA) using custom scripts and incorporating functions from EEGLAB (Delorme and Makeig, 2004). The EEG data was filtered between 0.5 and 200 Hz (4th order Butterworth FIR, zero-phase shift) with additional notch filters to reduce line noise (50 Hz) and its harmonics (100 and 150 Hz). Highly contaminated channels were identified by visual inspection and removed (7.4 ± 4.4 channels). The remaining channels were re-referenced to the common average. A list of single-trial responses created during data acquisition was used for trial exclusion due to unsuccessful task performance (i.e., stepping: 0.7 ± 1.2 trials, feet-in-place: 15.1 ± 7.8 trials).

2.4.2. Estimation of source-level activity

We used independent component analysis (ICA) and equivalent current dipole source localization to separate the high-density EEG into cortical source-level activity (Gramann et al., 2014; Makeig et al., 2009) and to reduce the influence of other sources of physiological noise (e.g., electromyogram and electrocardiogram) (Gwin et al., 2010; Kline et al., 2015; Oliveira et al., 2016). This approach is in line with previous studies on cortical dynamics during whole-body movement (Gwin et al., 2011; Sipp et al., 2013; Wagner et al., 2012, 2016).

A copy of the preprocessed EEG data was segmented according to a trigger for platform movement in the interval −5 to 2 s relative to the onset of the platform movement. This excluded the time intervals where the cue was presented to the participants and when the platform returned to the starting position. The EEG segments were visually inspected for non-stereotyped artifacts (e.g., cable movements), which were discarded. The remaining clean EEG segments were processed with CUDAICA (Raimondo et al., 2012), an implementation of Infomax independent component analysis (Makeig et al., 1996) for the graphics processing unit. The independent component analysis finds a set of spatial filters that separates the scalp recordings into maximally independent components (ICs) representing spatially stationary electrocortical processes (Makeig et al., 2004; Onton et al., 2006).

An equivalent current dipole was fitted to the scalp projection of each IC to estimate the location of its cortical source. The equivalent current dipoles were found using an standardized three-shell boundary element head model and standard electrode positions (DIPFIT toolbox within EEGLAB, (Delorme et al., 2012; Oostenveld and Oostendorp, 2002)). This procedure resulted in dipole locations inside a standard head model (MNI). Only the ICs whose scalp projection could be explained by a dipole inside the head with residual variance lower or equal to 10% were further analyzed. ICs related to eye movements and muscle artifacts were identified through visual inspection of the topography of its scalp projection, the spatial location of its associated equivalent current dipole, and its power spectral density. ICs related to brain activity (typical EEG power spectra and equivalent current dipole located inside of the head and with low residual variance) were further analyzed.

The ICs from all participants were clustered according to the spatial location of their associated equivalent current dipole, their power spectral density (between 2 and 48 Hz), and the topography of their scalp projection. The clustering routine relied on principal component analysis and the k-means algorithm to find clusters of ICs that are quantitatively similar. The number of clusters was selected as the largest number of clusters such that one cluster was located near the vertex and included at least one IC from each participant. This criterion was used because previous EEG studies on standing balance control have reported the most prominent responses over midline central scalp areas overlaying the SMA (Bolton, 2015; Varghese et al., 2017). Only clusters that included ICs from more than half of the participants were further considered. The set of spatial filters resulting from the independent component analysis, their associated current dipoles, and the cluster labels were stored for further analysis of the continuous preprocessed EEG data.

2.4.3. Event-related spectral perturbations

Oscillatory dynamics were quantified as relative changes in the power of intrinsic cortical rhythms according to the definition of event-related spectral perturbations (ERSP) (Makeig, 1993). After applying the spatial filters to the continuous preprocessed EEG data, single-trial responses were segmented between −1 and 8 s relative to cue onset. Trials with unsuccessful task performance were excluded from the analysis (see section 2.4.1 Preprocessing), and trials with residual muscle artifacts were further removed (average per participant: stepping: 1.7 ± 4.7 trials, feet-in-place: 2 ± 2 trials). The remaining number of trials per participant was on average 47.4 ± 5.1 trials in the stepping condition (range: 34–50 trials) and 32.9 ± 7.3 trials in the feet-in-place condition (range: 20–41 trials).

Single-trial spectrograms were computed and time-warped to normalize the duration of the response preparation phase (to the median duration across participants, using linear interpolation). Average log-transformed spectrograms showing relative power changes were computed per IC and response condition as the average difference between each (log transformed) single-trial spectrogram and the average (log transformed) spectrum within a baseline period (1 s window preceding cue onset). Average time-frequency maps for a given IC cluster were computed by averaging across the maps corresponding to the ICs members of the cluster, separately for each response condition.

2.4.4. Event-related potentials

For comparison with previous studies, we computed event-related potentials for each IC cluster and each response condition. We obtained source-level time-warped single-trial perturbation-related responses (as detailed in the previous section) and averaged across trials from the same IC and response condition. Average ERPs for a given IC cluster were computed by averaging across ERPs corresponding to ICs members of a given cluster (separately for each response condition). The objective of this analysis was to complement existing literature on perturbation-related potentials.

2.4.5. Cortical dynamics related to asymmetric postural behavior

The different postural behavior of stepping and feet-in-place responses was assessed by comparing the vertical load on each leg during the response execution phase. The vertical load was extracted from the force plate data in segments of four seconds centered around the perturbation onset. Changes in the vertical load were calculated with respect to a reference period between 2 and 1.5 s before the perturbation onset. The relative vertical load was computed for the swing and support body sides, and averaged across participants for each body side and

response condition. A comparison of the relative vertical load between swing and support body sides was used to evaluate the symmetry of postural behavior. Stepping responses are distinguished by asymmetric load distribution of the swing and support body sides, in contrast to symmetric load distribution during feet-in-place responses (McIlroy and Maki, 1993a, 1993b).

We expected cortical mediation of reactive balance responses during the later phases of the balance responses, following the early automatic postural responses that are likely coordinated at spinal and subcortical levels (Jacobs and Horak, 2007; Taube et al., 2006). Postural adjustments preceding voluntary and reactive stepping may be controlled by basal ganglia-thalamo-cortical loops, where the main cortical contributors are the SMA and the lateralized M1/S1 (Massion, 1992; Ng et al., 2013). Thus, cortical oscillatory dynamics related to the vertical load of swing and support body sides were evaluated by comparing the lateralized M1/S1 activity. Noteworthy, this analysis compared the swing and support body sides *within* each response condition.

2.5. Statistical analyses

Differences between response conditions were evaluated with surrogate statistics (Maris and Oostenveld, 2007; Nichols and Holmes, 2002). First, we computed the t-statistic between response conditions in the original dataset. Here we used two-tailed paired t-tests for the comparisons within clusters and two-tailed independent samples *t*-test (assuming unequal variance, Satterthwaite's approximation for effective degrees of freedom implemented in the *ttest2.m* Matlab function) for the comparison between lateralized M1/S1 clusters within single conditions. Then, we created surrogate data by randomly shuffling the condition labels (1000 iterations) and computing a surrogate t-statistic after each iteration. Finally, we compared the original t-statistic against the distribution of the surrogate statistics. We considered a significant difference if the original t-statistic laid beyond the tails of the distribution of surrogate statistics ($\alpha = 0.05$, two-tailed). We corrected the p-values associated with significant t-statistics for false discovery rate (FDR) at the same significance level (Benjamini and Yekutieli, 2001). We applied this evaluation for group-level statistical significance of the time-frequency ERSP maps and the time samples of the ERPs. Because our primary metrics are the time-frequency maps, we report mean difference maps with overlaid contours for uncorrected and FDR corrected p-values.

Differences in the time course of ERPs, power modulations, and the relative vertical load were assessed via bootstrap confidence intervals (1000 iterations, $\alpha = 0.05$). Significant differences from zero (or baseline) occur when the upper and lower confidence intervals of a given condition have the same sign. Significant differences between conditions were considered when the confidence intervals of the individual conditions did not overlap. If this was the case, we looked up the statistics for a specific time or time-frequency interval in the surrogate statistics results and reported the median t-statistic and median p-value.

3. Results

3.1. Clusters of independent components

We found seven IC clusters that contained independent components from more than half of the participants. Table 1 presents the Talairach coordinates of the cluster centroids. These coordinates provide an approximation to the localization of the actual cortical sources, limited by the spatial resolution of the source localization methods (standard electrode positions and standard head model). Five clusters were located along the sagittal midline and two clusters were lateralized to the left and right hemispheres. ICs belonging to two participants who stepped with the left foot were removed from the lateralized clusters, to prevent that brain asymmetry possibly associated with footedness interfered with the analyses (Elias et al., 1998; Peter and Durding, 1979; Willems et al., 2014).

Table 1
Estimated location of the cluster centroids.

IC cluster	Talairach coordinates (x, y, z)	Cortical location	Brodmann area
Midline central	−1, 0, 53	Supplementary motor area	BA6
Left central	−37, −16, 40	Left sensorimotor cortex	BA4
Right central	35, −5, 46	Right sensorimotor cortex	BA6
Midline parietal	6, −33, 56	Posterior parietal cortex	BA5
Midline occipital	5, −70, 17	Secondary visual cortex	BA18
Midline anterior prefrontal	−5, 40, −6	Anterior prefrontal cortex	BA10
Midline prefrontal	−11, 28, 28	Anterior cingulate cortex	BA32

3.2. Event-related spectral perturbation

Fig. 3 shows the average time-frequency maps per cluster and response condition, together with the maps of the mean difference between conditions. In the midline central cluster, located in the SMA, we found statistically significant differences between stepping and feet-in-place conditions for the frequency bands 6–9 Hz, 9–13 Hz, and 31–34 Hz. In other IC clusters the time-frequency maps revealed power modulations below 30 Hz and different from baseline that were largely similar in both response conditions. To summarize the power modulations across frequencies, Fig. 4 shows the average ERSP spectra during the cue observation (0–2 s), response preparation (2–5.6 s), and response execution (early: 5.6–6.1 s; late: 6.1–7 s) phases. Noteworthy, the response execution phase is separated in two consecutive segments. The first segment covers the first 500 ms after perturbation onset, corresponding with early cortical activity that may represent initial modulations of the medium- and long-latency postural responses (Bolton, 2015; Jacobs and Horak, 2007; Maki and McIlroy, 2007). The second segment covers the rest of the response execution phase, when successful reactive responses are completed.

We further analyzed the time course of power modulations for frequency bands showing significant differences in the midline central cluster, and for general frequency bands corresponding with theta (3–7 Hz), alpha (8–12 Hz), beta I (13–17 Hz), and beta II (18–25 Hz) rhythms in all other IC clusters. Fig. 4 shows the correspondence between these frequency bands and the average ERSP spectra. Fig. 5 shows the time course of selected frequency bands per IC cluster.

3.2.1. Distinct oscillatory dynamics between stepping and feet-in-place responses

Significant differences occurred in the midline central cluster for theta, alpha, and low-gamma rhythms (see Figs. 3 and 5). Stronger cortical activation occurred in trials with feet-in-place responses during the cue observation and response preparation phases, but not during the response execution phase. Following an initial suppression (power decrease) of the theta and alpha rhythms, a brief but significant partial enhancement of these rhythms appeared shortly after cue onset in trials with stepping responses (theta: median $t(13) = 4.23$, $p = 0.001$; alpha: median $t(13) = 4.21$, $p = 0.001$). Afterwards, suppression of the low-gamma rhythm occurred in trials with feet-in-place responses (median $t(13) = 4.03$, $p = 0.0014$). The suppression of the alpha and low-gamma rhythms that appeared during the cue observation phase, was maintained for a substantial part of the response preparation phase, indicating stronger cortical activation for feet-in-place responses (alpha: median $t(13) = 4.39$, $p = 0.0007$ and $t(13) = 4.73$, $p = 0.0004$; low-gamma: median $t(13) = 4.20$, $p = 0.001$ and $t(13) = 4.14$, $p = 0.0012$).

In several clusters, comparisons between response conditions were significant after the surrogate statistics (i.e., the null-hypothesis can be

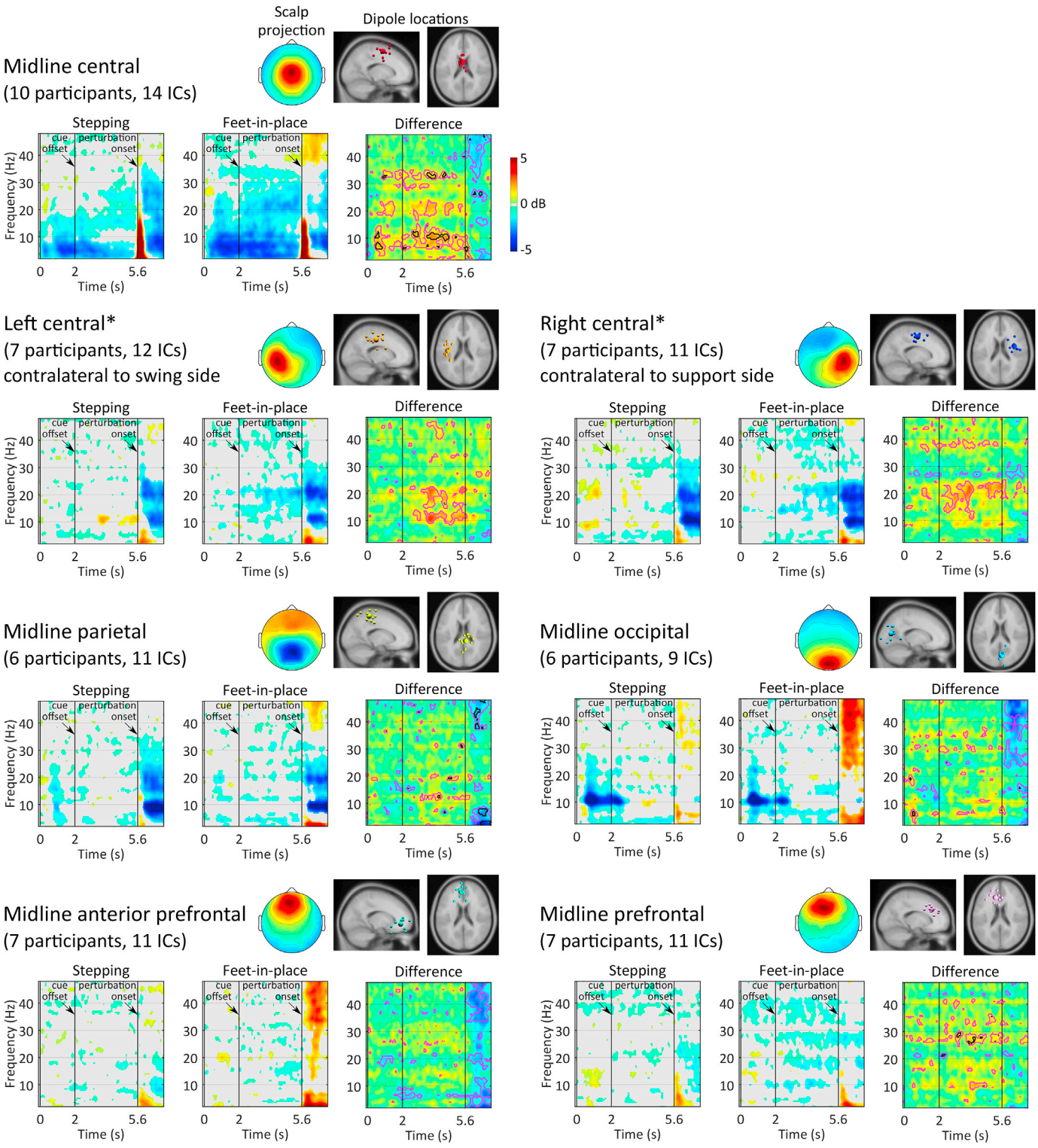

Fig. 3. *Event-related spectral perturbations time-frequency maps.* The *Stepping* and *Feet-in-place* time-frequency maps show the mean power decrease (shown in blue) and power increase (shown in red) for each response condition. Power modulations not significantly different from baseline (1 s segment preceding cue onset) are masked with gray color. The *Difference* time-frequency map shows the mean difference (*Stepping* minus *Feet-in-place*) between conditions. Contour lines indicate differences between conditions with a critical $\alpha < 0.05$ before (magenta) and after (black) correction for false discovery rate. The graphics on the right of each cluster label present the scalp projection of each cluster centroid, the estimated location of the individual equivalent current dipoles for all cluster members (small spheres), and the estimated location of the cluster centroid (larger sphere). Solid vertical lines indicate cue onset (0 s), cue offset (2 s), and perturbation onset (group median latency: 5.6 s). *The left and right central clusters only included ICs of participants who stepped with the right leg ($n = 8$).

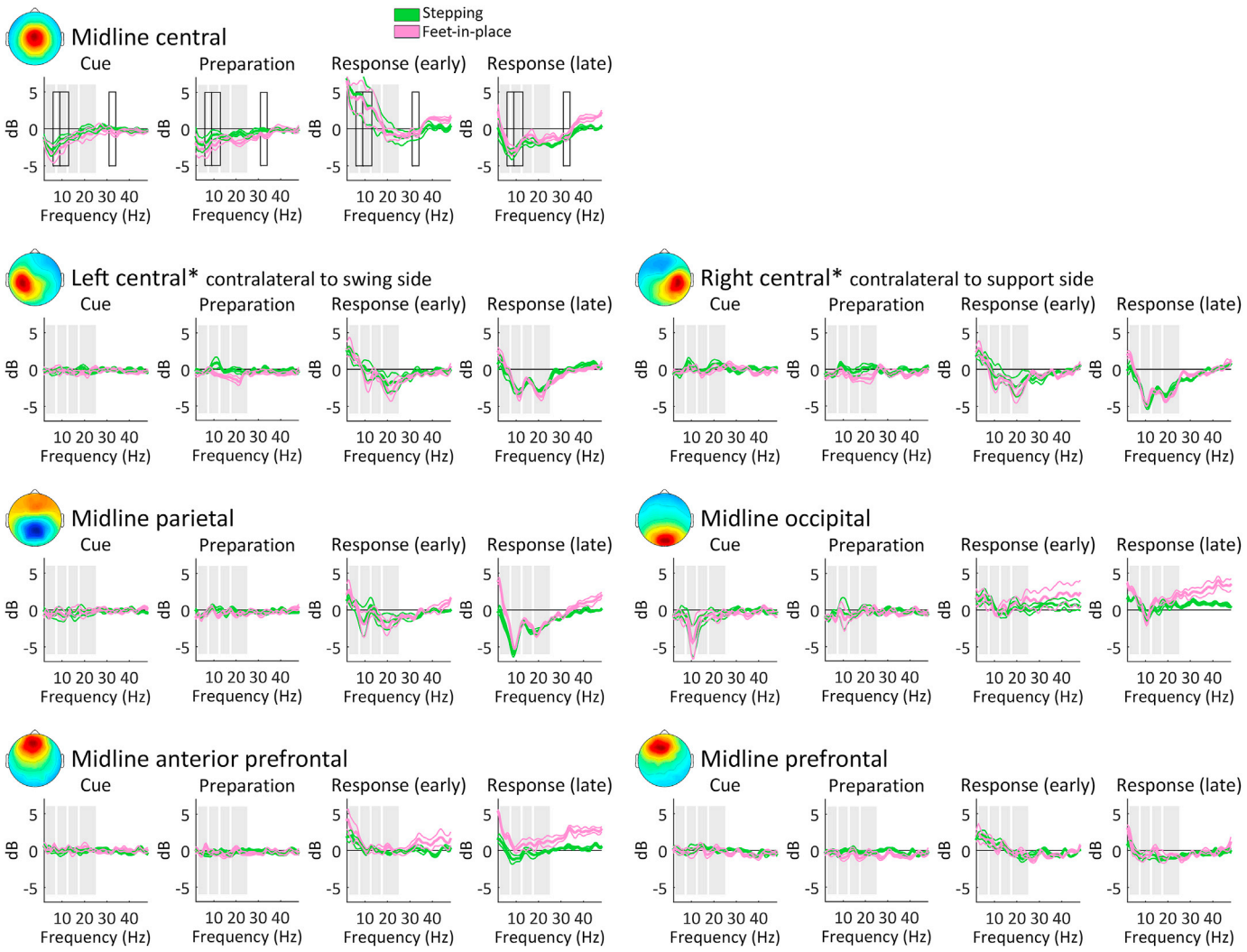

Fig. 4. *Summary of event-related spectral perturbations across frequencies.* Each plot shows the mean ERSP spectra during the cue observation (0–2 s), response preparation (2–5.6 s), and response execution (early: 5.6–6.1 s; late: 6.1–7 s) phases. Power modulations of multiple cortical rhythms occurred in all IC clusters for trials requiring stepping (green) or feet-in-place (pink) responses. Gray shaded areas indicate the general frequency bands used in further analyses: 3–7 Hz, 8–12 Hz, 13–17 Hz, and 18–25 Hz. Black outlines shown for the midline central cluster indicate the frequency bands with significant differences between response conditions (after correction for false discovery rate): 6–9 Hz, 9–13 Hz, and 31–34 Hz *The left and right central clusters only included ICs of participants who stepped with the right leg (n = 8).

rejected), but did not survive the stringent correction for false discovery rate (see Fig. 5). Because there is a risk to bias our analysis toward false negatives, we briefly mention these uncorrected differences as noteworthy trends:

- Midline anterior prefrontal cluster: stronger, long-lasting enhancement of the theta rhythm during the response execution phase, in trials with feet-in-place responses (median $t(10) = -2.43$, $p = 0.035$, uncorrected).
- Midline central cluster: stronger suppression of the beta II rhythm during the response preparation phase, in trials with feet-in-place responses (median t(13) between 2.37 and 2.52, p between 0.025 and 0.034, uncorrected).
- Left central cluster: weak alpha suppression (feet-in-place responses) contrasting sustained alpha enhancement (stepping responses) during the response preparation phase (median t(11) between 2.35 and 3.05, p between 0.011 and 0.038, uncorrected).
- Right central cluster: early beta I suppression during the response preparation phase in trials with feet-in-place responses (median t(9) between 2.41 and 2.85, p between 0.019 and 0.039, uncorrected).
- Left/right central clusters: beta II suppression slowly increasing toward the end of the response preparation phase in trials with feet-in-place responses (left: median $t(11) = 2.55$, $p = 0.027$, uncorrected; right: median $t(9) = 3.03$, $p = 0.014$, uncorrected).

3.2.2. *Common oscillatory dynamics underlying stepping and feet-in-place responses*

During the cue observation phase, the midline occipital cluster presented strong alpha suppression after cue onset, which disappeared shortly after cue offset at the beginning of the response preparation phase. The same cluster showed brief beta I and beta II suppression accompanying the initial alpha suppression, but returning to baseline levels before cue offset. The midline parietal cluster presented similar brief suppression of the theta, beta I, and beta II rhythms following cue onset. During the response preparation phase, multiple cortical rhythms were suppressed in the midline parietal cluster and the left and right central clusters. At the beginning of this phase, brief suppression of the beta rhythms appeared in the left central cluster (beta I) and the midline parietal cluster (beta II), accompanying the return to baseline of the cue-related alpha suppression in the midline occipital cluster. Intermittent suppression of the theta (midline parietal, and left and right central

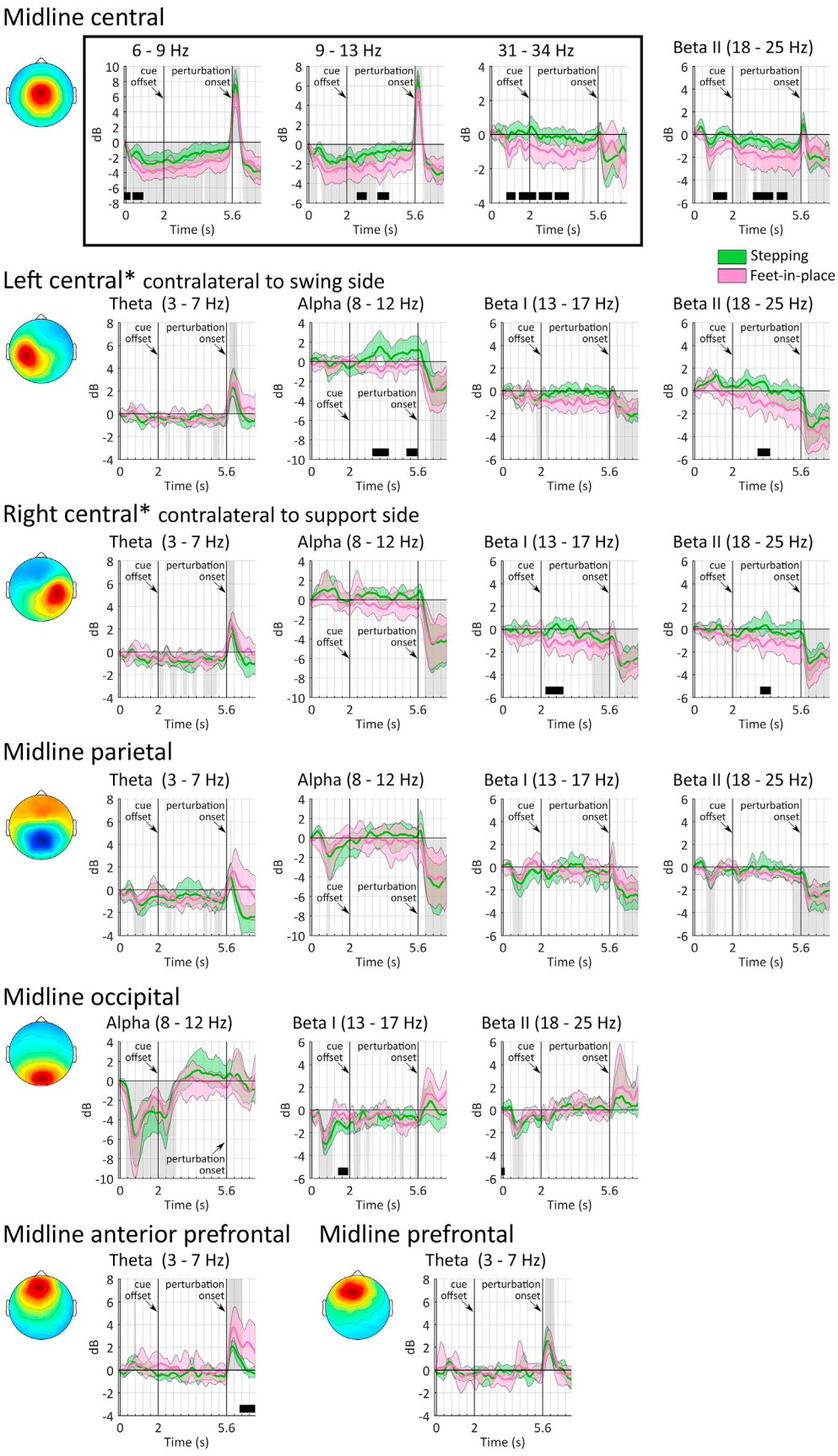

Fig. 5. *Time course of power modulations for specific frequency bands.* These plots show mean power modulations (and the 95% confidence intervals) elicited in each cluster during trials using stepping (green) and feet-in-place (pink) responses. Note that for the midline central cluster (located in the SMA) the boxed time course plots correspond with significant differences (after correction for false discovery rate) between conditions (6–9 Hz, 9–13 Hz, and 31–34 Hz). All other time course plots correspond with general frequency bands defined in this study. Solid vertical lines indicate cue onset (0 s), cue offset (2 s), and perturbation onset (group median latency: 5.6 s). The vertical grid represents intervals of 400 ms (after time warping). Gray areas indicate significant differences from baseline (positive: power increase; negative: power decrease) concurrent in both response conditions. Black markers at the bottom of each axis indicate a trend toward significant differences between response conditions ($p < 0.05$, uncorrected). *The left and right central clusters only included ICs of participants who stepped with the right leg ($n = 8$).

clusters) and beta I (midline occipital) rhythms occurred throughout the response preparation phase. Near the end of this phase, stronger suppression of the beta rhythms occurred in the right central cluster (beta I) and the midline parietal cluster (beta II).

During the response execution phase, directly after perturbation onset, a brisk broadband enhancement of theta, alpha, and beta I rhythms appeared in the midline central cluster. At the same time, brisk enhancement of the theta rhythm occurred in the midline anterior prefrontal cluster, the midline prefrontal cluster, the midline parietal cluster, and the left and right central clusters. In the midline central cluster, the brief broadband enhancement was followed by an overall suppression of all cortical rhythms, which was sustained for the rest of the response execution phase, when whole-body movement takes place. The execution of reactive balance responses also elicited sustained suppression of the

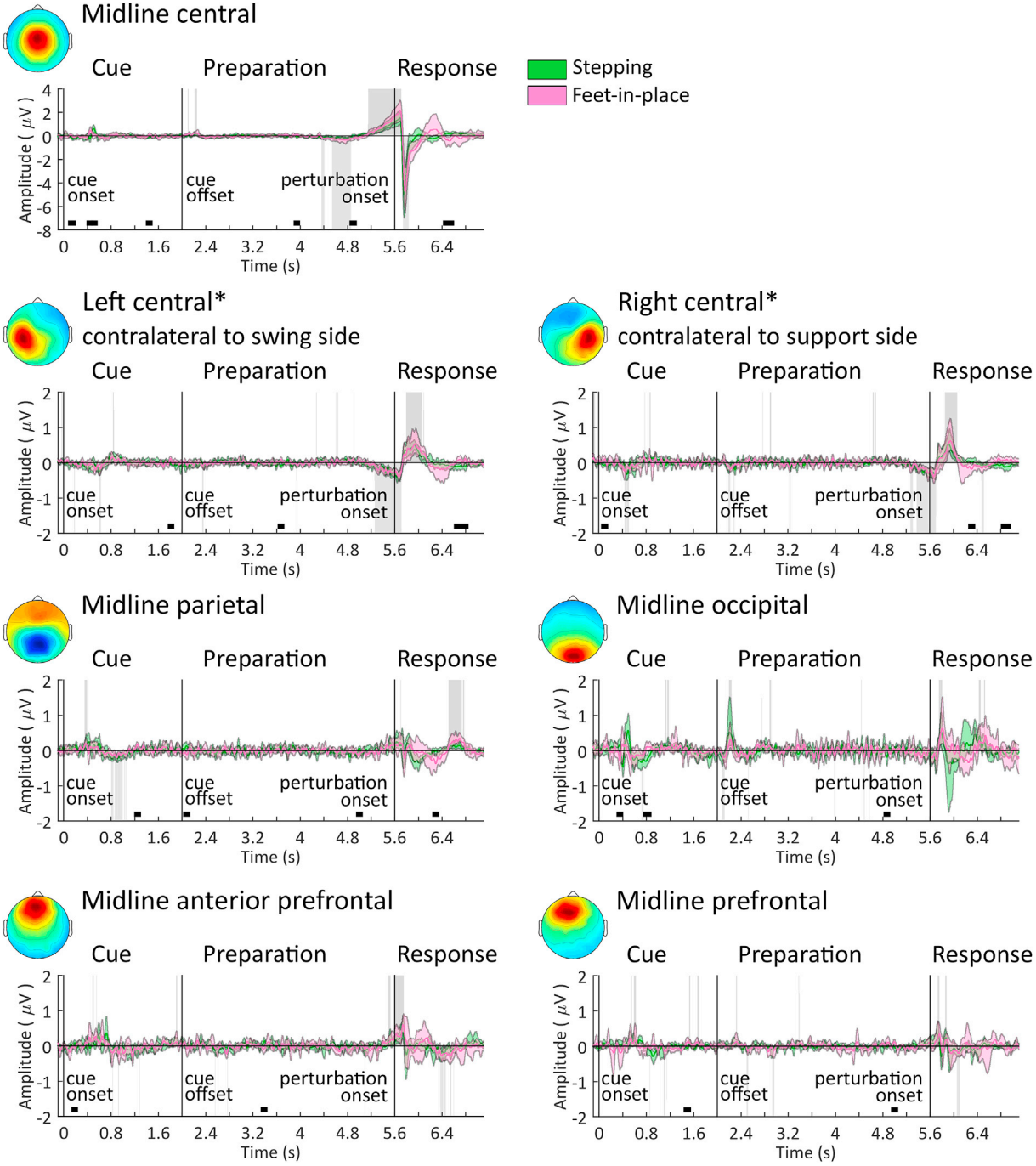

Fig. 6. *Event-related potentials.* The plots show the 95% confidence intervals for the ERP elicited in each cluster in during trials using stepping (green) and feet-in-place (pink) responses. The ERP in the midline central cluster, located in the SMA, shows the characteristics of perturbation-related potentials (Varghese et al., 2017), i.e., contingent negative variation (CNV) and P1 and N1 potentials. Noteworthy, the morphology of the CNV is altered here due to the use of a high-pass filter with cut-off frequency at 0.5 Hz. Other IC clusters (midline anterior prefrontal, midline parietal, and left and right central) also present indications of CNV and P1-N1 potentials during the response preparation and response execution phases. Solid vertical lines indicate cue onset (0 s), cue offset (2 s), and perturbation onset (group median latency: 5.6 s). The vertical grid represents intervals of 400 ms (after time warping). Gray shaded areas indicate significant differences from zero concurrent in both response conditions. Black markers at the bottom of each axis indicate a trend towards significant differences between response conditions ($p < 0.05$, uncorrected). *The left and right central clusters only included ICs of participants who stepped with the right leg ($n = 8$).

alpha, beta I, and beta II rhythms in the midline parietal cluster and the left and right central clusters.

3.3. Event-related potentials

Fig. 6 shows the ERPs in each IC cluster for both response conditions. Except for brief episodic differences in the midline occipital and left central clusters, we found no significant differences between response conditions in the time interval from 0 to 500 ms following the perturbation onset. The most prominent potentials occurred in the midline central cluster, with the largest amplitudes after perturbation onset. The ERP in the midline central cluster showed the characteristics of perturbation-related potentials (Bolton, 2015; Varghese et al., 2017), i.e., a slow potential shift preceding the perturbation onset (around 1.2 s), followed by P1 (80 ms) and N1 (150 ms) potentials after the perturbation onset. Several previous EEG studies on balance control (Fujiwara et al., 2011; Jacobs et al., 2008; Mochizuki et al., 2008, 2010; Smith et al., 2012) have reported that expectation of an upcoming balance perturbation elicits a negative potential shift known as contingent negative variation (CNV), which is associated with cortical mechanisms of motor

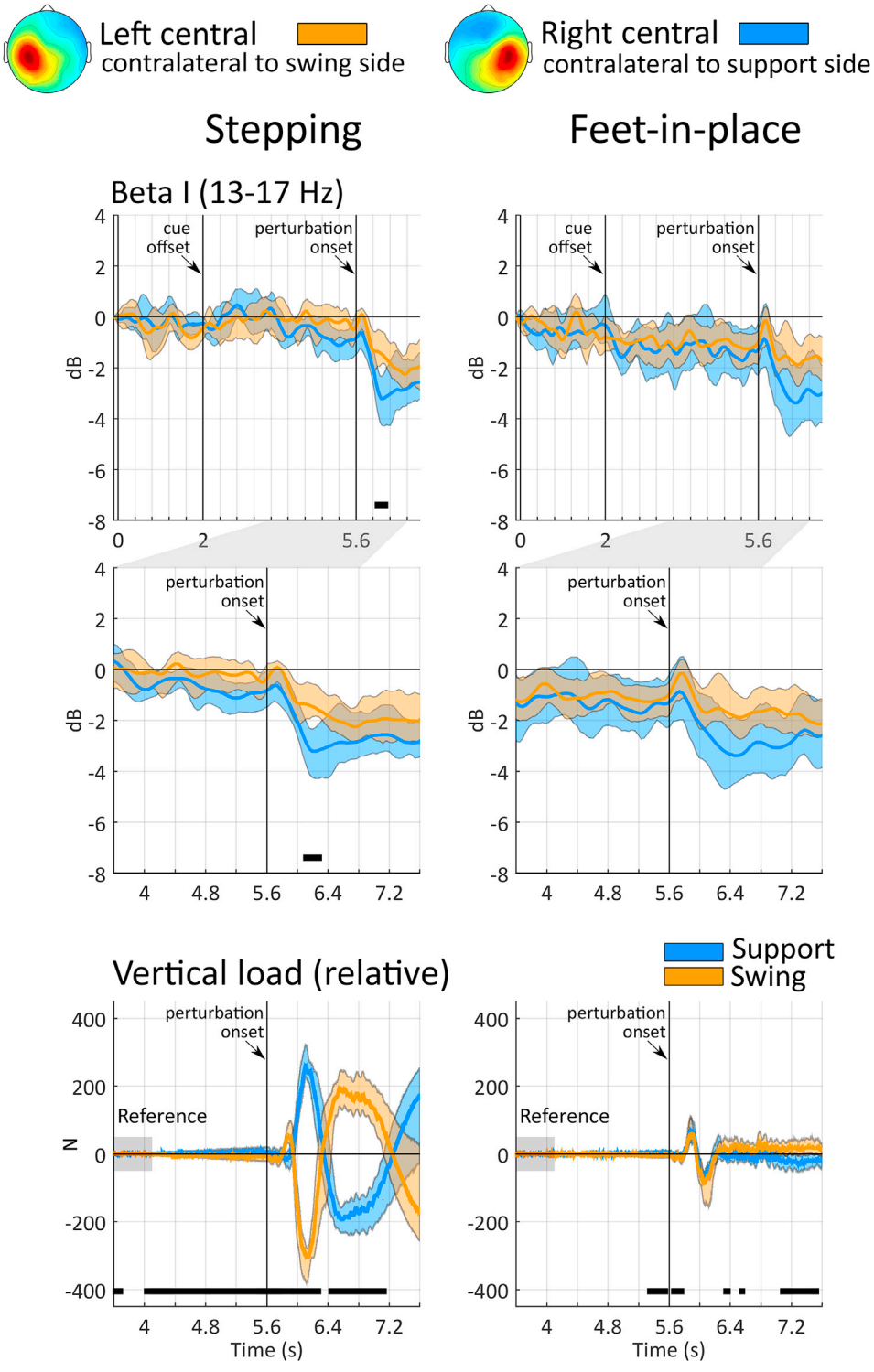

Fig. 7. *Asymmetric activation of the sensorimotor cortices and changes in vertical load during stepping responses.* Modulations of the beta (13–17 Hz) rhythm in the left and right central IC clusters, corresponding to the sensorimotor cortices contralateral to the swing (orange) and support (blue) sides. The bottom plots show the relative change in vertical load during an interval of ±2 s around perturbation onset (baseline: −2 to −1.5 s). Stepping responses (left column) show a typical asymmetric vertical loading pattern (i.e. preparatory postural adjustment) preceding step initiation (0–400 ms after perturbation onset), followed by increased load on the support side during the actual step. Feet-in-place responses (right column) show symmetric load of swing and support sides, as expected. Strong beta suppression in the sensorimotor cortex contralateral to the support body side coincided with the maximum vertical load of the support body side. The vertical grid represents intervals of 400 ms (after time warping). The curves show the 95% confidence intervals. Black markers at the bottom of the plots indicate that the confidence intervals do not overlap. Importantly, these clusters only include ICs of participants who stepped with the right leg (n = 8).

preparation (Neuper and Pfurtscheller, 2001; van Rijn et al., 2011). Noteworthy, the morphology of the CNV shown in Fig. 6 differs from previous reports due to the use of a higher cut-off frequency for the high-pass filter (0.5 Hz) during preprocessing. Additional potential shifts preceding the perturbation onset were found in the left and right central clusters and the midline anterior prefrontal cluster. In the midline anterior prefrontal cluster the potential shift returned to zero around 150 ms after the perturbation, coinciding with the latency of the N1 potential in the midline central cluster. In the left and right central clusters, the potential shift was also terminated around 150 ms and it was followed by a positive potentials peaking around 300 ms.

3.3.1. Cortical dynamics related to postural behavior

Fig. 7 shows different modulation of the beta I rhythm in the left and right central clusters, with respect to the relative vertical load of the swing and support body sides. Importantly, these comparisons only considered the participants who stepped with their right foot (swing body side) in trials requiring stepping responses ($n = 8$).

The stepping responses corresponded with asymmetric vertical load of the swing and support sides, whereas the feet-in-place responses corresponded with symmetric vertical load. Irrespectively of the response condition, vertical load gradually shifted toward the support side during the response preparation phase. Asymmetric modulation of the beta I rhythm occurred in trials with stepping responses. The right central cluster (contralateral to the support body side) showed stronger beta I suppression (median $t = 2.199$, $p = 0.043$; the effective degrees of freedom varied between 10 and 20, according to the estimated variances of each time-frequency bin), which coincided with the maximum vertical load of the support body side (~500 ms). Modulations of other cortical rhythms showed symmetric cortical activation of the left and right central clusters for both response conditions.

4. Discussion

We determined oscillatory activity of multiple cortical areas during preparation and execution of reactive balance responses, with particular interest in differences between stepping and feet-in-place responses. The distinct postural demand of these responses corresponded with differential modulations of theta, alpha, and low-gamma rhythms in the SMA. Higher postural demand, associated with feet-in-place responses, was reflected in stronger power modulations during preparatory, but not reactive balance control. Translations of the support surface elicited perturbation-related potentials arising from the SMA, with additional sources in PFC, and bilateral M1/S1. The balance perturbations also elicited broadband power increase in SMA, and enhancement of the theta rhythm in PFC, ACC, PPC, and bilateral M1/S1. Remarkably, the distinct whole-body movements and postural demands of the stepping and feet-in-place responses resulted in largely similar oscillatory dynamics during the response execution phase, with two notable differences: reactive feet-in-place responses corresponded with stronger theta enhancement in PFC, and, during reactive stepping, asymmetric vertical load during single support corresponded with stronger beta suppression in M1/S1 contralateral to the support leg. Overall, our results provide novel insights into the cortical mechanisms that underlie the control of human standing balance and upright posture.

4.1. Preparatory balance control

4.1.1. Integration of visual information

Contextual information given by visual cues may be transmitted via visuo-parieto-frontal projections to the SMA for selection of optimal motor programs (Scott, 2004; Takakusaki, 2013). In our study, this was indicated by suppression of oscillatory activity (Figs. 3–5) in the (secondary) visual cortex (alpha and beta rhythms), PPC (theta and beta rhythms), and SMA (theta, alpha, and beta rhythms). This interpretation is in line with studies indicating that theta and alpha rhythms are related to early stages of visual processing (Klimesch, 1999), that the alpha rhythm directs information toward task-relevant neural structures (Klimesch et al., 2011), and that the beta rhythm may mediate information between visual and sensorimotor systems (Pavlidou et al., 2014; Wróbel, 2000).

4.1.2. Selection of motor programs and preparatory cortical activation

Suppression of theta, alpha, and low-gamma rhythms in the SMA during cue observation and response preparation corresponded with the postural demand of the two response conditions (Figs. 3 and 5). Stronger suppression reflected the higher postural demand of the feet-in-place responses at two different time intervals.

During the cue observation phase, partial enhancement of the theta and alpha rhythms in the SMA may represent an update of motor programs after the visual cue indicated the use of stepping responses. This would imply that a feet-in-place response (high postural demand) was selected as the default motor program, which needed to be updated when a stepping response (low postural demand) was required. Indeed, a previous study reported that when uncertainty about postural demand exists, the central nervous system is conservatively driven toward a default preparatory state in anticipation of high postural demand (Mochizuki et al., 2010). Consistent with our results, stopping action or changing a motor program induces brief enhancement of theta/alpha rhythms over multiple cortical areas, including (pre)SMA (Jha et al., 2015).

Later during the cue observation phase, low-gamma suppression specifically occurred after clear definition of a trial with high postural demand. This low-gamma suppression continued through the first half of the response preparation phase, together with the alpha suppression that started earlier during the cue observation phase. The cerebral cortex is thought to regulate the activity of subcortical postural centers, to (indirectly) modify postural responses according to environmental demands and task constraints (Jacobs and Horak, 2007; Nutt et al., 2011). Top-down modulation of movement appears to involve synchronization between distant neuronal networks in frequencies above 20 Hz, corresponding to beta and gamma rhythms (Engel et al., 2001). During preparation of motor responses, the power of cortical oscillations between 13 and 35 Hz is strongly suppressed (Crone et al., 1998; Neuper and Pfurtscheller, 2001; Pfurtscheller and Lopes da Silva, 1999), while (phase) synchronization with surface EMG is increased (Chen et al., 1998; Schoffelen et al., 2011). In contrast, increased amplitude of beta (and low-gamma) oscillations may serve to maintain the current postural set at the expense of slowing new movements (Engel and Fries, 2010), and the selective suppression of these rhythms appears to be related to the selection or inhibition of competing responses (van Wijk et al., 2009). Our results show cortical activity during the response preparation phase that differentiates the postural demand of these two response conditions. We speculate that the alpha and low-gamma suppression may be related to the upregulation of subcortical postural centers and the priming of the motor system to react to the balance perturbation.

Additional results suggest cortical mechanisms of motor preparation during both response conditions, akin to the preparation of many other types of movement (Shibasaki, 2012). Specifically, we observed alpha and beta suppression (SMA, PPC, and bilateral M1/S1 in SMA) and CNV (SMA, PFC, and bilateral M1/S1), during the response preparation phase (Figs. 3–5). Previous studies have shown that prior knowledge about perturbation onset (Jacobs et al., 2008; Mochizuki et al., 2008) and perturbation characteristics (Fujiwara et al., 2011; Mochizuki et al., 2010; Smith et al., 2012), modulates the amplitude/magnitude of scalp-level fronto-central CNV and the suppression of mid-central alpha/beta rhythms. Yet, we did not observe significant differences in CNV or alpha/beta suppression, even though information about postural demand and perturbation characteristics was known in advance. Thus, we consider that these results mainly represent general mechanisms of response preparation.

Beyond scalp level analyses in previous studies, our results

demonstrate multiple cortical areas engaged in visual and cognitive processing following the visual stimuli indicating the requested response. Interestingly, the CNV latencies suggest sequential activation of SMA, followed by the bilateral M1/S1, and later the PFC. Consistent with this result, it has been suggested that the SMA recruits action- and perception-related areas for processing of subsequent movements (Gómez et al., 2003).

4.2. Reactive balance control

4.2.1. Detecting and monitoring challenges to postural stability

The perturbation onset elicited broadband enhancement of SMA theta, alpha, and beta rhythms, concurrent with multifocal theta enhancement in ACC, PFC, PPC, and bilateral M1/S1 (Figs. 3–5), and perturbation-related potentials in SMA and bilateral M1/S1 (Fig. 6). These results were common to both response conditions.

The broadband enhancement in the SMA could represent top-down processes related to the detection of an event that challenges postural stability, i.e., the detection of an unexpected event. Our results show brief broadband enhancement that generalizes between responses with distinct postural demand and behavior. Brief fronto-central broadband enhancement has also been reported following minimal challenges to postural stability that can be easily overcome using feet-in-place responses (Mierau et al., 2017; Varghese et al., 2014, 2015). Furthermore, studies relying on ERP-based analyses have shown that the amplitude of the N1 potential is reduced when the onset of a balance perturbation is predictable (Adkin et al., 2006, 2008; Mochizuki et al., 2010). To link these results, it is important to mention that Varghese et al. (2014) showed the correspondence between N1 potentials and a broadband power increase (explained through phase-locking) that closely matches the results presented here. Thus, we favor the interpretation of detection of a challenge to postural stability over other processes commonly associated with SMA activity (e.g., movement initiation). However, it cannot be ruled out that the broadband enhancement in the SMA may also represent contributions to other aspects of balance control.

The multifocal theta enhancement could represent the activity of a cortical network involved in monitoring the current postural stability state. Its emergence following perturbation onset is consistent with fronto-centro-parietal theta enhancement previously reported in conditions of transient and sustained compromised postural stability (Hülsdünker et al., 2015; Mierau et al., 2017; Slobounov et al., 2009). Multifocal enhancement of the theta rhythm has also been reported during loss of balance while walking on a balance beam (Sipp et al., 2013), starting during the last gait cycle preceding loss of balance and continuing until stable gait was achieved, providing further support for the suggested functional significance of theta enhancement in monitoring the stability state. Interestingly, we observed stronger and longer-lasting enhancement of the theta rhythm in PFC during feet-in-place responses (Figs. 3 and 5). Previous studies suggest that the PFC participates in the detection of errors and novel events (Wessel et al., 2012), as well as a subsequent inhibition of motor responses (Wessel and Aron, 2013). This suggest that the stronger theta rhythm during feet-in-place responses may indicate an ongoing process of motor inhibition to suppress an “automatic” reactive stepping response (which would be the more natural response to high-intensity mechanical perturbations).

A variety of novel and unexpected events are associated with modulations of the midline frontal theta rhythm (Cavanagh and Frank, 2014), resembling the modulations found in our study. In earlier studies (Adkin et al., 2006; Dimitrov et al., 1996), it was quickly noticed that perturbation-related potentials bared resemblance with the error-related negativity that is present during performance errors in a variety of reaction-time tasks (Gehring et al., 1993, 2018), and it was proposed that the cortical perturbation-related responses represented an error in stability. Although direct comparison of ERPs, and the anatomical localization of their equivalent current dipoles, between balance perturbations and a flanker task suggested different cortical sources for the two conditions (Marlin et al., 2014), it is worth revisiting the possible functional meaning of the perturbation-related responses. In particular, the strong SMA broadband power increase and the multifocal enhancement of the theta rhythm should be considered as possible nodes of a cortico-subcortical network that implements top-down response inhibition (Wessel and Aron, 2017).

Although our focus is on oscillatory dynamics, we performed an additional ERP-based analysis to complement the existing literature. First, we present further evidence of the likely cortical source of perturbation-related potentials. The N1 potential is strongly represented in the SMA, with additional small but consistent potentials in PFC and bilateral M1/S1. Second, the perturbation-related potentials elicited in both postural demand conditions were indistinguishable. Thus, the N1 potential could represent the processing of sensory input (which was identical in both conditions) or the detection of a challenge to postural stability (i.e., unexpected events). Yet a relation with other functions (e.g., movement initiation) cannot be excluded (Varghese et al., 2017). In the bilateral M1/S1, late perturbation-related potentials (~300 ms) are consistent with re-afferent potentials following voluntary and passive movements (Kornhuber and Deecke, 1965). Further analyses with respect to the different kinematics of these two response conditions are necessary to better determine the functional meaning of early and late perturbation-related potentials.

4.2.2. Lateralization of cortical activity during balance responses

Stronger beta suppression occurred in M1/S1 contralateral to the support body side in stepping trials, coinciding with the period of maximum vertical load (Fig. 7). In contrast, there was no apparent difference between bilateral M1/S1 beta ERD in feet-in-place trials. Despite the clearly different movements involved in stepping and feet-in-place responses, we only found subtle differences in the modulation of the cortical beta rhythm. A relative power decrease of the sensorimotor rhythms is typically associated with an active sensorimotor cortex, related to increased sensory input or efferent motor commands (Neuper and Pfurtscheller, 1992; Pfurtscheller, 2003). Moreover, suppression of the central alpha and beta rhythms can be related to increased cortical excitability (Laaksonen et al., 2012; Parkkonen et al., 2015) and increased excitability of the corticospinal tract (Chen et al., 1998). Noteworthy, our analyses were solely based on power modulations and phase information was not analyzed in any way. Thus, the common modulations of cortical sensorimotor alpha and beta rhythms in SMA, PPC, and bilateral M1/S1 during both reactive balance control responses may still contribute to the control of muscle activity via neural synchronization, as corticomuscular connectivity can occur without associated power modulations (Bastos and Schoffelen, 2016). In line with a recent study demonstrating unidirectional cortical drive to leg muscles during gait (Artoni et al., 2017), future studies may focus on quantifying directional corticomuscular connectivity to further determine the cortical control of reactive balance responses (Mima and Hallett, 1999; Yang et al., 2017).

Alternatively, we consider the possibility that the central nervous system (brain, cerebellum, basal ganglia, brainstem, and spinal cord) may control coordinated movements during quiet stance and gait by specifying the co-activation of groups of muscles, known as muscle synergies (Ivanenko et al., 2006) and their recruitment. In this view, the subtle differences are perhaps not surprising in light of a previous study reporting common recruitment of multiple standing-leg muscle synergies for stepping and feet-in-place responses (Chvatal et al., 2011). Noteworthy, only one muscle synergy was found to be specific for stepping. We must emphasize that, although the results of Chvatal et al. (2011) suggest a high degree of similarity between the neural control of the two distinct responses, it is an open debate whether or not muscle synergies have a corresponding neuroanatomical representation in the central nervous system (Bizzi and Cheung, 2013; Flash and Bizzi, 2016). However, accumulating evidence suggests that the human cerebral cortex is at

least partly involved in the flexible recruitment of muscle synergies (Cheung et al., 2012; Godlove et al., 2016; Scano et al., 2017). Indeed, a recent study on postural control (de Kam et al., 2018) reported that feet-in-place responses to multidirectional balance perturbations were consistently represented with three muscle synergies in healthy individuals, but the muscle synergies were less consistent in individuals with chronic stroke, with one muscle synergy even being undetectable in nearly half of the participants with stroke. Interestingly, the absent muscle synergy involved muscles with typical long-latency responses, which argues in favor of cortical involvement in the control of long-latency postural responses. Based on these observations, we speculate that the lateralized beta suppression in stepping trials may reflect direct cortical involvement in recruiting a stepping-specific muscle synergy for stabilization during single support, although processing of asymmetric motor output or sensory input to/from the support leg cannot be excluded as an alternative explanation.

5. Conclusions

Our study presents novel insights into the cortical dynamics of SMA, PFC, and M1/S1 during the control of human balance. The SMA may be involved in preparatory balance control, as evidenced by the differential modulations of alpha and low-gamma rhythms, showing increased SMA activation for reactive balance responses with higher postural demand. We speculate that the increased SMA activation could be related to the modulation of subcortical postural circuits. In addition, the SMA may participates in the detection of a challenge to postural stability, as indicated by broadband power increase of theta, alpha, and beta rhythms, without apparent differentiation between the specific type of response. The PFC may be involved in monitoring the state of postural stability or inhibiting an automatic stepping response, as indicated by stronger and longer lasting power increase of the theta rhythm for reactive balance responses with higher postural demand (feet-in-place responses). The bilateral M1/S1 may participate in postural stabilization, with subtle differences in power modulation of the sensorimotor beta rhythm for symmetric and asymmetric reactive balance responses. Noteworthy, our conclusions are drawn from analyses on power modulations of EEG-derived source-level cortical activity. Complementary analyses on cortico-cortical and corticomuscular phase synchronization can provide valuable information on the direct effect of cerebral cortex on balance and posture. Understanding the cortical mechanisms of human balance control is instrumental for the development of novel treatments to prevent falls and related injuries due to aging or neurological conditions (e.g., stroke and Parkinson's disease).

Funding

This work was supported by the European Research Council (FP7/2007–2013) ERC grant agreement n. 291339, project “4DEEG: A new tool to investigate the spatial and temporal activity patterns in the brain”; by the Dutch Technology Foundation (STW) NeuroSIPE n. 10737, project “BalRoom”; and by a Netherlands Organisation for Scientific Research, VIDI grant to Dr. Weerdesteyn n. 91717369, project “Roads to recovery”. Funding sources were not involved in study design; in the collection, analysis and interpretation of data; in the writing of this report; nor in the decision to submit the article for publication.

Declarations of interest

None.

Appendix A. Supplementary data

Supplementary data to this article can be found online at https://doi.org/10.1016/j.neuroimage.2018.12.045.

References

Adkin, A.L., Campbell, A.D., Chua, R., Carpenter, M.G., 2008. The influence of postural threat on the cortical response to unpredictable and predictable postural perturbations. Neurosci. Lett. 435, 120–125.
Adkin, A.L., Quant, S., Maki, B.E., McIlroy, W.E., 2006. Cortical responses associated with predictable and unpredictable compensatory balance reactions. Exp. Brain Res. 172, 85.
Artoni, F., Fanciullacci, C., Bertolucci, F., Panarese, A., Makeig, S., Micera, S., Chisari, C., 2017. Unidirectional brain to muscle connectivity reveals motor cortex control of leg muscles during stereotyped walking. Neuroimage 159, 403–416.
Basar, E., Basar-Eroglu, C., Karakas, S., Schurmann, M., 1999. Oscillatory brain theory: a new trend in neuroscience. IEEE Eng. Med. Biol. Mag. 18, 56–66.
Bastos, A.M., Schoffelen, J.-M., 2016. A tutorial review of functional connectivity analysis methods and their interpretational pitfalls. Front. Syst. Neurosci. 9.
Benjamini, Y., Yekutieli, D., 2001. The control of the false discovery rate in multiple testing under dependency. Ann. Stat. 1165–1188.
Bizzi, E., Cheung, V.C., 2013. The neural origin of muscle synergies. Front. Comput. Neurosci. 7.
Bohnen, N.I., Jahn, K., 2013. Imaging: what can it tell us about parkinsonian gait? Mov. Disord. 28, 1492–1500.
Bolton, D., 2015. The role of the cerebral cortex in postural responses to externally induced perturbations. Neurosci. Biobehav. Rev. 57, 142–155.
Buzsáki, G., Anastassiou, C.A., Koch, C., 2012. The origin of extracellular fields and currents — EEG, ECoG, LFP and spikes. Nat. Rev. Neurosci. 13, 407.
Cavanagh, J.F., Frank, M.J., 2014. Frontal theta as a mechanism for cognitive control. Trends Cognit. Sci. 18, 414–421.
Chen, R., Yaseen, Z., Cohen, L.G., Hallett, M., 1998. Time course of corticospinal excitability in reaction time and self-paced movements. Ann. Neurol. 44, 317–325.
Cheung, V.C., Turolla, A., Agostini, M., Silvoni, S., Bennis, C., Kasi, P., Paganoni, S., Bonato, P., Bizzi, E., 2012. Muscle synergy patterns as physiological markers of motor cortical damage. Proc. Natl. Acad. Sci. U. S. A. 109, 14652–14656.
Chvatal, S.A., Torres-Oviedo, G., Safavynia, S.A., Ting, L.H., 2011. Common muscle synergies for control of center of mass and force in nonstepping and stepping postural behaviors. J. Neurophysiol. 106, 999–1015.
Crone, N.E., Miglioretti, D.L., Gordon, B., Sieracki, J.M., Wilson, M.T., Uematsu, S., Lesser, R.P., 1998. Functional mapping of human sensorimotor cortex with electrocorticographic spectral analysis. I. Alpha and beta event-related desynchronization. Brain 121, 2271–2299.
de Kam, D., Geurts, A.C., Weerdesteyn, V., Torres-Oviedo, G., 2018. Direction-specific instability poststroke is associated with deficient motor modules for balance control. Neurorehabilitation Neural Repair 32, 655–666.
de Kam, D., Kamphuis, J.F., Weerdesteyn, V., Geurts, A.C.H., 2016. The effect of weight-bearing asymmetry on dynamic postural stability in healthy young individuals. Gait Posture 45, 56–61.
Delorme, A., Makeig, S., 2004. EEGLAB: an open source toolbox for analysis of single-trial EEG dynamics including independent component analysis. J. Neurosci. Methods 134, 9–21.
Delorme, A., Palmer, J., Onton, J., Oostenveld, R., Makeig, S., 2012. Independent EEG sources are dipolar. PLoS One 7.
Dietz, V., Quintern, J., Berger, W., 1984. Cerebral evoked potentials associated with the compensatory reactions following stance and gait perturbation. Neurosci. Lett. 50, 181–186.
Dietz, V., Quintern, J., Berger, W., Schenck, E., 1985. Cerebral potentials and leg muscle e.m.g. responses associated with stance perturbation. Exp. Brain Res. 57, 348–354.
Dimitrov, B., Gavrilenko, T., Gatev, P., 1996. Mechanically evoked cerebral potentials to sudden ankle dorsiflexion in human subjects during standing. Neurosci. Lett. 208.
Elias, L.J., Bryden, M.P., Bulman-Fleming, M.B., 1998. Footedness is a better predictor than is handedness of emotional lateralization. Neuropsychologia 36, 37–43.
Engel, A.K., Fries, P., 2010. Beta-band oscillations—signalling the status quo? Curr. Opin. Neurobiol. 20, 156–165.
Engel, A.K., Fries, P., Singer, W., 2001. Dynamic predictions: oscillations and synchrony in top–down processing. Nat. Rev. Neurosci. 2, 704.
Flash, T., Bizzi, E., 2016. Cortical circuits and modules in movement generation: experiments and theories. Curr. Opin. Neurobiol. 41, 174–178.
Fujiwara, K., Kiyota, N., Maeda, K., 2011. Contingent negative variation and activation of postural preparation before postural perturbation by backward floor translation at different initial standing positions. Neurosci. Lett. 490, 135–139.
Gaetz, W., Edgar, J.C., Wang, D.J., Roberts, T.P.L., 2011. Relating MEG measured motor cortical oscillations to resting γ-Aminobutyric acid (GABA) concentration. Neuroimage 55, 616–621.
Gehring, W.J., Goss, B., Coles, M.G.H., Meyer, D.E., Donchin, E., 1993. A neural system for error detection and compensation. Psychol. Sci. 4, 385–390.
Gehring, W.J., Goss, B., Coles, M.G.H., Meyer, D.E., Donchin, E., 2018. The error-related negativity. Perspect. Psychol. Sci. 13, 200–204.
Godlove, J., Gulati, T., Dichter, B., Chang, E., Ganguly, K., 2016. Muscle synergies after stroke are correlated with perilesional high gamma. Annu. Clin. Transl. Neurol. 3, 956–961.
Gómez, C.M., Marco, J., Grau, C., 2003. Preparatory visuo-motor cortical network of the contingent negative variation estimated by current density. Neuroimage 20, 216–224.
Gramann, K., Ferris, D.P., Gwin, J.T., Makeig, S., 2014. Imaging natural cognition in action. Int. J. Psychophysiol. 91, 22–29.
Gwin, J.T., Gramann, K., Makeig, S., Ferris, D.P., 2010. Removal of movement artifact from high-density EEG recorded during walking and running. J. Neurophysiol. 103, 3526–3534.

Gwin, J.T., Gramann, K., Makeig, S., Ferris, D.P., 2011. Electrocortical activity is coupled to gait cycle phase during treadmill walking. Neuroimage 54, 1289–1296.
Hall, S.D., Stanford, I.M., Yamawaki, N., McAllister, C.J., Rönnqvist, K.C., Woodhall, G.L., Furlong, P.L., 2011. The role of GABAergic modulation in motor function related neuronal network activity. Neuroimage 56, 1506–1510.
Hamano, T., Lüders, H.O., Ikeda, A., Collura, T.F., Comair, Y.G., Shibasaki, H., 1997. The cortical generators of the contingent negative variation in humans: a study with subdural electrodes. Electroencephalogr. Clin. Neurophysiol. Evoked Potentials Sect. 104, 257–268.
Hülsdünker, T., Mierau, A., Neeb, C., Kleinöder, H., Strüder, H.K., 2015. Cortical processes associated with continuous balance control as revealed by EEG spectral power. Neurosci. Lett. 592, 1–5.
Ivanenko, Y.P., Poppele, R.E., Lacquaniti, F., 2006. Motor control programs and walking. Neuroscientist 12, 339–348.
Jacobs, J., Horak, F., 2007. Cortical control of postural responses. J. Neural. Transm. 114, 1339–1348.
Jacobs, J.V., 2014. Why we need to better understand the cortical neurophysiology of impaired postural responses with age, disease, or injury. Front. Integr. Neurosci. 8.
Jacobs, J.V., Fujiwara, K., Tomita, H., Furune, N., Kunita, K., Horak, F.B., 2008. Changes in the activity of the cerebral cortex relate to postural response modification when warned of a perturbation. Clin. Neurophysiol. 119, 1431–1442.
Jahn, K., Zwergal, A., 2010. Imaging supraspinal locomotor control in balance disorders. Restor. Neurol. Neurosci. 28, 105–114.
Jha, A., Nachev, P., Barnes, G., Husain, M., Brown, P., Litvak, V., 2015. The frontal control of stopping. Cerebr. Cortex 25, 4392–4406.
Klimesch, W., 1999. EEG alpha and theta oscillations reflect cognitive and memory performance: a review and analysis. Brain Res. Rev. 29, 169–195.
Klimesch, W., Fellinger, R., Freunberger, R., 2011. Alpha oscillations and early stages of visual encoding. Front. Psychol. 2.
Kline, J.E., Huang, H.J., Snyder, K.L., Ferris, D.P., 2015. Isolating gait-related movement artifacts in electroencephalography during human walking. J. Neural. Eng. 12, 046022.
Klostermann, F., Nikulin, V.V., Kuhn, A.A., Marzinzik, F., Wahl, M., Pogosyan, A., Kupsch, A., Schneider, G.H., Brown, P., Curio, G., 2007. Task-related differential dynamics of EEG alpha- and beta-band synchronization in cortico-basal motor structures. Eur. J. Neurosci. 25, 1604–1615.
Kornhuber, H.H., Deecke, L., 1965. Hirnpotentialänderungen bei Willkürbewegungen und passiven Bewegungen des Menschen: bereitschaftspotential und reafferente Potentiale. Pflugers Arch. für Gesamte Physiol. Menschen Tiere 284, 1–17.
Laaksonen, K., Kirveskari, E., Mäkelä, J.P., Kaste, M., Mustanoja, S., Nummenmaa, L., Tatlisumak, T., Forss, N., 2012. Effect of afferent input on motor cortex excitability during stroke recovery. Clin. Neurophysiol. 123, 2429–2436.
Magnus, R., 1926. Cameron Prize Lectures on some results of studies in the physiology of posture. Lancet 208, 585–588.
Makeig, S., 1993. Auditory event-related dynamics of the EEG spectrum and effects of exposure to tones. Electroencephalogr. Clin. Neurophysiol. 86, 283–293.
Makeig, S., Bell, A.J., Jung, T.P., Senjowski, T.J., 1996. Independent component analysis of electroencephalographic data. In: Touretzky, D., Mozer, M., Hasselmo, M. (Eds.), Advances in Neural Information Processing Systems, pp. 145–151.
Makeig, S., Debener, S., Onton, J., Delorme, A., 2004. Mining event-related brain dynamics. Trends in Cognit. Neurosci. 8, 204–210.
Makeig, S., Gramann, K., Jung, T.P., Sejnowski, T.J., Poizner, H., 2009. Linking brain, mind and behavior. Int. J. Psychophysiol. 73, 95–100.
Maki, B.E., McIlroy, W.E., 2007. Cognitive demands and cortical control of human balance-recovery reactions. J. Neural. Transm. 114, 1279–1296.
Maris, E., Oostenveld, R., 2007. Nonparametric statistical testing of EEG- and MEG-data. J. Neurosci. Methods 164, 177–190.
Marlin, A., Mochizuki, G., Staines, W.R., McIlroy, W.E., 2014. Localizing evoked cortical activity associated with balance reactions: does the anterior cingulate play a role? J. Neurophysiol. 111, 2634–2643.
Massion, J., 1992. Movement, posture and equilibrium: interaction and coordination. Prog. Neurobiol. 38, 35–56.
McIlroy, W., Maki, B., 1993a. Do anticipatory postural adjustments precede compensatory stepping reactions evoked by perturbation? Neurosci. Lett. 164, 199–202.
McIlroy, W.E., Maki, B.E., 1993b. Task constraints on foot movement and the incidence of compensatory stepping following perturbation of upright stance. Brain Res. 616, 30–38.
Mierau, A., Hülsdünker, T., Strüder, H.K., 2015. Changes in cortical activity associated with adaptive behavior during repeated balance perturbation of unpredictable timing. Front. Behav. Neurosci. 9, 272.
Mierau, A., Pester, B., Hülsdünker, T., Schiecke, K., Strüder, H.K., Witte, H., 2017. Cortical correlates of human balance control. Brain Topogr. 1–13.
Mima, T., Hallett, M., 1999. Corticomuscular coherence: a review. J. Clin. Neurophysiol. 16, 501–511.
Mochizuki, G., Boe, S., Marlin, A., McIlroy, W.E., 2010. Perturbation-evoked cortical activity reflects both the context and consequence of postural instability. Neuroscience 170, 599–609.
Mochizuki, G., Sibley, K.M., Cheung, H.J., Camilleri, J.M., McIlroy, W.E., 2009. Generalizability of perturbation-evoked cortical potentials: independence from sensory, motor and overall postural state. Neurosci. Lett. 451, 40–44.
Mochizuki, G., Sibley, K.M., Esposito, J.G., Camilleri, J.M., McIlroy, W.E., 2008. Cortical responses associated with the preparation and reaction to full-body perturbations to upright stability. Clin. Neurophysiol. 119, 1626–1637.
Muthukumaraswamy, S.D., 2010. Functional properties of human primary motor cortex gamma oscillations. J. Neurophysiol. 104, 2873–2885.
Muthukumaraswamy, S.D., 2014. The use of magnetoencephalography in the study of psychopharmacology (pharmaco-MEG). J. Psychopharmacol. 28, 815–829.
Neuper, C., Pfurtscheller, G., 1992. Event-related negativity and alpha band desynchronization in motor reactions. EEG-EMG Zeitschrift fur Elektroenzephalographie, Elektromyographie und verwandte Gebiete 23, 55–61.
Neuper, C., Pfurtscheller, G., 2001. Event-related dynamics of cortical rhythms: frequency-specific features and functional correlates. Int. J. Psychophysiol. 43, 41–58.
Ng, T.H.B., Sowman, P.F., Brock, J., Johnson, B.W., 2013. Neuromagnetic imaging reveals timing of volitional and anticipatory motor control in bimanual load lifting. Behav. Brain Res. 247, 182–192.
Nichols, T.E., Holmes, A.P., 2002. Nonparametric permutation tests for functional neuroimaging: a primer with examples. Hum. Brain Mapp. 15, 1–25.
Nonnekes, J., De Kam, D., Geurts, A.C., Weerdesteyn, V., Bloem, B.R., 2013. Unraveling the mechanisms underlying postural instability in Parkinson's disease using dynamic posturography. Expert Rev. Neurother. 13, 1303–1308.
Nutt, J.G., Horak, F.B., Bloem, B.R., 2011. Milestones in gait, balance, and falling. Mov. Disord. 26, 1166–1174.
Ohara, S., Ikeda, A., Kunieda, T., Yazawa, S., Baba, K., Nagamine, T., Taki, W., Hashimoto, N., Mihara, T., Shibasaki, H., 2000. Movement-related change of electrocorticographic activity in human supplementary motor area proper. Brain 123, 1203–1215.
Oliveira, A.S., Schlink, B.R., Hairston, W.D., König, P., Ferris, D.P., 2016. Induction and separation of motion artifacts in EEG data using a mobile phantom head device. J. Neural. Eng. 13, 036014.
Onton, J., Westerfield, M., Townsend, J., Makeig, S., 2006. Imaging human EEG dynamics using independent component analysis. Neurosci. Biobehav. Rev. 30, 808–822.
Oostenveld, R., Oostendorp, T.F., 2002. Validating the boundary element method for forward and inverse EEG computations in the presence of a hole in the skull. Hum. Brain Mapp. 17, 179–192.
Oostenveld, R., Praamstra, P., 2001. The five percent electrode system for high-resolution EEG and ERP measurements. Clin. Neurophysiol. 112, 713–719.
Parkkonen, E., Laaksonen, K., Piitulainen, H., Parkkonen, L., Forss, N., 2015. Modulation of the~ 20-Hz motor-cortex rhythm to passive movement and tactile stimulation. Brain and behavior 5.
Pavlidou, A., Schnitzler, A., Lange, J., 2014. Distinct spatio-temporal profiles of beta-oscillations within visual and sensorimotor areas during action recognition as revealed by MEG. Cortex 54, 106–116.
Peter, M., Durding, B.M., 1979. Footedness of left- and right-handers. Am. J. Psychol. 92, 133–142.
Peterson, D.S., Horak, F.B., 2016. Neural control of walking in people with parkinsonism. Physiology 31, 95–107.
Pfurtscheller, G., 2003. Induced oscillations in the alpha band: functional meaning. Epilepsia 44, 2–8.
Pfurtscheller, G., Lopes da Silva, F.H., 1999. Event-related EEG/MEG synchronization and desynchronization: basic principles. Clin. Neurophysiol. 110, 1842–1857.
Quant, S., Adkin, A.L., Staines, W.R., McIlroy, W.E., 2004. Cortical activation following a balance disturbance. Exp. Brain Res. 155, 393–400.
Raimondo, F., Kamienkowski, J.E., Sigman, M., Slezak, D.F., 2012. CUDAICA: GPU optimization of infomax-ICA EEG analysis. Comput. Intell. Neurosci. 2010, 206972 .
Rektor, I., Bareš, M., Brázdil, M., Kaňovský, P., Rektorová, I., Sochůrková, D., Kubová, D., Kuba, R., Daniel, P., 2005. Cognitive-and movement-related potentials recorded in the human basal ganglia. Mov. Disord. 20, 562–568.
Scano, A., Chiavenna, A., Malosio, M., Molinari Tosatti, L., Molteni, F., 2017. Muscle synergies-based characterization and clustering of poststroke patients in reaching movements. Front. Bioeng. Biotechnol. 5, 62-62.
Schoffelen, J.-M., Poort, J., Oostenveld, R., Fries, P., 2011. Selective movement preparation is subserved by selective increases in corticomuscular gamma-band coherence. J. Neurosci. 31, 6750.
Scott, S.H., 2004. Optimal feedback control and the neural basis of volitional motor control. Nat. Rev. Neurosci. 5, 532–546.
Sherrington, C.S., 1910. Flexion-reflex of the limb, crossed extension-reflex, and reflex stepping and standing. J. Physiol. 40, 28–121.
Shibasaki, H., 2012. Cortical activities associated with voluntary movements and involuntary movements. Clin. Neurophysiol. 123, 229–243.
Sipp, A.R., Gwin, J.T., Makeig, S., Ferris, D.P., 2013. Loss of balance during balance beam walking elicits a multifocal theta band electrocortical response. J. Neurophysiol. 110, 2050–2060.
Slobounov, S., Cao, C., Jaiswal, N., Newell, K.M., 2009. Neural basis of postural instability identified by VTC and EEG. Exp. Brain Res. 199, 1–16.
Smith, B.A., Jacobs, J.V., Horak, F.B., 2012. Effects of magnitude and magnitude predictability of postural perturbations on preparatory cortical activity in older adults with and without Parkinson's disease. Exp. Brain Res. 222, 455–470.
Smith, B.A., Jacobs, J.V., Horak, F.B., 2014. Effects of amplitude cueing on postural responses and preparatory cortical activity of people with Parkinson's disease. J. Neurol. Phys. Ther.: J. Neurol. Phys. Ther. 38, 207.
Staines, W.R., McIlroy, W.E., Brooke, J.D., 2001. Cortical representation of whole-body movement is modulated by proprioceptive discharge in humans. Exp. Brain Res. 138.
Takakusaki, K., 2013. Neurophysiology of gait: from the spinal cord to the frontal lobe. Mov. Disord. 28, 1483–1491.
Takakusaki, K., 2017. Functional neuroanatomy for posture and gait control. J. Mod. Dynam. 10, 1–17.
Taube, W., Schubert, M., Gruber, M., Beck, S., Faist, M., Gollhofer, A., 2006. Direct corticospinal pathways contribute to neuromuscular control of perturbed stance. J. Appl. Physiol. 101, 420–429, 1985.

van Rijn, H., Kononowicz, T., Meck, W., Ng, K.K., Penney, T., 2011. Contingent negative variation and its relation to time estimation: a theoretical evaluation. Front. Integr. Neurosci. 5.
van Wijk, B.C., Daffertshofer, A., Roach, N., Praamstra, P., 2009. A role of beta oscillatory synchrony in biasing response competition? Cerebr. Cortex 19, 1294–1302.
Varghese, J.P., Beyer, K.B., Williams, L., Miyasike-daSilva, V., McIlroy, W.E., 2015. Standing still: is there a role for the cortex? Neurosci. Lett. 590, 18–23.
Varghese, J.P., Marlin, A., Beyer, K, B., Staines, W.R., Mochizuki, G., McIlroy, W.E., 2014. Frequency characteristics of cortical activity associated with perturbations to upright stability. Neurosci. Lett. 578, 33–38.
Varghese, J.P., McIlroy, R.E., Barnett-Cowan, M., 2017. Perturbation-evoked potentials: significance and application in balance control research. Neurosci. Biobehav. Rev. 83, 267–280.
Wagner, J., Makeig, S., Gola, M., Neuper, C., Müller-Putz, G., 2016. Distinct β band oscillatory networks subserving motor and cognitive control during gait adaptation. J. Neurosci. 36, 2212–2226.
Wagner, J., Solis-Escalante, T., Grieshofer, P., Neuper, C., Müller-Putz, G.R., Scherer, R., 2012. Level of participation in robotic-assisted treadmill walking modulates midline sensorimotor EEG rhythms in able-bodied subjects. Neuroimage 63, 1203–1211.
Wessel, J.R., Aron, A.R., 2013. Unexpected events induce motor slowing via a brain mechanism for action-stopping with global suppressive effects. J. Neurosci. 33, 18481.
Wessel, J.R., Aron, A.R., 2017. On the globality of motor suppression: unexpected events and their influence on behavior and cognition. Neuron 93, 259–280.
Wessel, J.R., Danielmeier, C., Morton, J.B., Ullsperger, M., 2012. Surprise and error: common neuronal architecture for the processing of errors and novelty. J. Neurosci. 32, 7528.
Willems, R.M., der Haegen, L.V., Fisher, S.E., Francks, C., 2014. On the other hand: including left-handers in cognitive neuroscience and neurogenetics. Nat. Rev. Neurosci. 15, 193–201.
Wittenberg, E., Thompson, J., Nam, C.S., Franz, J.R., 2017. Neuroimaging of human balance control: a systematic review. Front. Hum. Neurosci. 11.
Wróbel, A., 2000. Beta activity: a Carrier for visual attention. Acta Neurobiol. Exp. 60, 247–260.
Yang, Y., Dewald, J.P.A., van der Helm, F.C.T., Schouten, A.C., 2017. Unveiling neural coupling within the sensorimotor system: directionality and nonlinearity. Eur. J. Neurosci. 48, 2407–2415.